

This is the peer reviewed version of the following article:

Changes in dermal fibroblasts from Abcc6^{-/-} mice are present before and after the onset of ectopic tissue mineralization / Boraldi, Federica; Bartolomeo, Angelica; Li, Q.; Uitto, J.; Quaglino, Daniela. - In: JOURNAL OF INVESTIGATIVE DERMATOLOGY. - ISSN 0022-202X. - STAMPA. - 134:7(2014), pp. 1855-1861. [10.1038/jid.2014.88]

Terms of use:

The terms and conditions for the reuse of this version of the manuscript are specified in the publishing policy. For all terms of use and more information see the publisher's website.

10/01/2026 20:11



Changes in dermal fibroblasts from Abcc6^{-/-} mice are present before and after the onset of ectopic tissue mineralization

Journal:	<i>Journal of Investigative Dermatology</i>
Manuscript ID:	JID-2013-0943.R2
Manuscript Type:	Original Article
Date Submitted by the Author:	n/a
Complete List of Authors:	Boraldi, Federica; University of Modena and Reggio Emilia, Life Sciences Bartolomeo, Angelica; University of Modena and Reggio Emilia, Life Sciences Li, Qiaoli; Thomas Jefferson University, Dermatology and Cutaneous Biology Uitto, Jouni; Thomas Jefferson University, Dermatology and Cutaneous Biology Quaglino, Daniela; University of Modena and Reggio Emilia, Dept. Biomedical Sciences
Key Words:	Pseudoxanthoma elasticum, elastin, fibroblasts, ectopic calcification, connective tissue

Changes in dermal fibroblasts from Abcc6^{-/-} mice are present before and after the onset of ectopic tissue mineralization

¹Federica Boraldi, ¹Angelica Bartolomeo, ²Qiaoli Li, ²Jouni Uitto and ¹Daniela Quaglino

¹Department of Life Sciences, University of Modena and Reggio Emilia, Modena (Italy)

²Department of Dermatology and Cutaneous Biology, Thomas Jefferson University, Philadelphia (USA)

Running title: fibroblasts in the PXE mouse model

Abbreviations: ABCC6/Abcc6, ATP – binding cassette sub-family C member 6 (human/mouse); Ank, progressive ankylosis protein; Bmp2, bone morphogenic protein 2; Enpp1, pyrophosphatase/phosphodiesterase 1; KO, knock out; Opn, osteopontin; Pi, inorganic phosphate; PPi, inorganic pyrophosphate; PXE, Pseudoxanthoma elasticum; ROS, reactive oxygen species; Tnap, tissue non-specific alkaline phosphatase; WT, wild type.

Address for correspondence:

Prof. Daniela Quaglino
Department of Life Sciences
University of Modena and Reggio Emilia
Via Campi 287 41125 Modena (Italy)
Phone: ++39-0592055418
Fax: ++39-0592055426
Email: quaglino.daniela@unimore.it

Abstract

Pseudoxanthoma elasticum (PXE), a rare genetic disease caused by mutations in the ABCC6 gene, is characterized by progressive calcification of elastic fibers in the skin, eyes and the cardiovascular system. The pathomechanisms of the mineralization is still obscure. Several hypotheses have been proposed, one of them suggesting a role for fibroblasts in controlling the amount and the quality of the calcified extracellular matrix. This hypothesis raises the question whether changes in mesenchymal cells are the cause and/or the consequences of the calcification process. In this study, fibroblasts were isolated and cultured from Abcc6^{+/+} and Abcc6^{-/-} mice of different ages in order to investigate parameters known to be associated with the phenotype of fibroblasts from PXE patients. Results demonstrate few changes (Ank and Opn down-regulation) are already present before the occurrence of calcification. By contrast, a modification of other parameters (intracellular O₂⁻ content, Tnap activity and Bmp2 up-regulation) can be observed in Abcc6^{-/-} mice after the onset of tissue mineralization. These data suggest that in the Abcc6^{-/-} genotype, dermal fibroblasts actively contribute to changes that promote matrix calcification and that these cells can be further modulated with time by the calcified environment, thus contributing to the age-dependent progression of the disease.

Introduction

Pseudoxanthoma elasticum (PXE) is a hereditary disease caused primarily by mutations in the ABCC6 gene (Bergen et al., 2000; Le Saux et al., 2000, Ringpfeil et al., 2000), yet the mechanisms leading to elastic fiber mineralization and consequently to clinical manifestations are not well understood. A number of hypotheses have been proposed in order to explain how lack or impaired function of ABCC6, a transmembrane transporter protein, almost exclusively expressed in the liver, can cause alterations in peripheral soft connective tissues, including elastic fiber calcification in the skin, eyes and the arterial blood vessels (Quaglino et al., 2011; Li et al., 2012). It has been proposed that ABCC6 transporter deficiency may alter the availability of circulating factors, presumably metabolized and secreted by the liver, which are physiologically required to prevent aberrant calcifications and are able to modulate the phenotype of mesenchymal cells, such as fibroblasts (Ronchetti et al., 2013). As a consequence of fibroblasts' abnormal protein profile (Boraldi et al., 2009), extracellular matrix components are differentially synthesized and/or degraded and elastic fiber mineralization ensues (Contri et al., 1996, Passi et al., 1996; Quaglino et al., 2005; Gheduzzi et al., 2007). Alternatively, it has been suggested that, serum factors controlling soft connective tissue calcification are abnormally secreted by the liver and cause the calcification of elastic fibers. If this is the case, changes in the characteristics of mesenchymal cells could represent a secondary response to the mineralized environment (Le Saux et al., 2006). A number of studies has been performed demonstrating that PXE fibroblasts, even though isolated from patient's tissues and cultured in an optimal in vitro environment, maintain a number of characteristics that clearly discriminate pathologic from healthy cells (Ronchetti et al., 2013). Nevertheless, it is currently unclear which changes in fibroblasts occur before mineralization of elastic fibers and might be considered pathogenic for calcification, and which changes represent the cellular response to the mineralized environment. So far, all in vitro investigations on PXE have been performed on fibroblasts isolated and cultured from patients, i.e., from individuals who have been diagnosed on the basis of clinical manifestations as a consequence of calcification. Taking advantage of the PXE

animal model, which recapitulates the PXE phenotype, including the slow progression of tissue mineralization (Gorgels et al., 2005; Klement et al., 2005), the aim of this study was to compare fibroblasts from congenic *Abcc6*^{-/-} (KO) and *Abcc6*^{+/+} (WT) mice. Since calcification in these animals occurs only after 5-6 weeks of age (Klement et al., 2005), fibroblasts were isolated from KO and WT mice at the age of 0.5 (absence of calcification) and 12 months (presence of calcification). A set of cellular parameters we have previously shown to be altered in dermal fibroblasts from PXE patients and to be related to the mineralization have been investigated (Boraldi et al., 2009; Boraldi et al., 2013). Therefore, cells were characterized for their proliferative capabilities and for their redox balance (Quaglino et al., 2000; Pasquali-Ronchetti et al., 2006), looking at the intracellular content of reactive oxygen species (ROS). Moreover, the expression of proteins exerting a key role on the development of ectopic calcification (Giachelli et al., 2005), such as bone morphogenic protein 2 (Bmp2), osteopontin (Opn), pyrophosphatase/phosphodiesterase 1 (Enpp1), progressive ankylosis protein (Ank), and tissue non-specific alkaline phosphatase (Tnap), was evaluated by Western blot analysis and Tnap activity (Boraldi et al., 2013) was assessed by spectrophotometry.

Results

Fibroblast proliferation capabilities

The number of fibroblasts that can be isolated from the skin of mice is progressively lower with advancing age, and therefore a higher number of adult animals was necessary in order to avoid differences in the number of population doublings of fibroblasts from young and older animals during all experimental procedures. In contrast to human dermal fibroblasts, murine cells reach senescence around passage 4. Therefore, fibroblasts, independently from their genotype, were studied only at passages 2 to 3. Nevertheless, fibroblasts isolated from the skin of adult mice have a lower capacity to replicate in vitro compared to cells from younger animals and, when observed by phase contrast microscopy, appeared larger with cytoplasmic vacuoles (Figure 1A). Differences in

the proliferation capabilities were independent from the genotype but were clearly related to animal's age (Figure 1 B).

Intracellular ROS content

Since aging is characterized by an altered redox balance and an oxidative stress has been demonstrated in PXE either in vitro or in vivo, both in patients and in animal models (Pasquali-Ronchetti et al., 2006; Garcia et al., 2008; Li et al., 2008), the intracellular ROS content was evaluated in mouse fibroblasts. Figure 2 shows that the H₂O₂ content is not affected by age nor by the genotype. Interestingly, there was no difference in the amount of superoxide anion in fibroblasts from young WT and KO mice, whereas there was a significant increase in O₂⁻ in fibroblasts from adult Abcc6^{-/-} mice compared to cells grown from WT animals of the same age or from younger Abcc6^{-/-} mice (Figure 2).

Protein expression

No differences in Bmp2 expression were observed in young WT and KO animals (i.e. before the occurrence of calcification). With age, a significant upregulation was observed only in cells grown from adult KO animals (Figure 3).

Evaluation of Tnap protein expression revealed a significant increase with mice age, without differences between WT and KO animals (Figure 4). Similarly, Tnap activity was significantly upregulated in fibroblasts from adult compared to younger mice (Figure 4). Moreover, enzymatic activity was even higher (p<0.05) in cells from adult KO mice compared to WT mice of the same age (Figure 4).

In murine dermal fibroblasts, Enpp1 expression was significantly decreased in adult mice as compared to young animals, however, no differences were observed between Abcc6^{-/-} and Abcc6^{+/+} mice (Figure 5).

On the contrary, Abcc6^{-/-} mice, at all ages, were characterized by a significantly lower expression of

Ank compared to WT animals. However, no changes were noted between cells from young and adult animals (Figure 5), indicating that this protein is not affected by animal's age.

Osteopontin, a well known inhibitor of the calcification process, was significantly reduced in *Abcc6*^{-/-} fibroblasts compared to cells from age-matched WT mice. Differences were negligible with age (Figure 6), indicating that mouse genotype is the main regulator of Opn expression.

Conclusions

While we have made significant progress in understanding the molecular basis of PXE, pathogenic mechanisms responsible for the calcification of elastic fibers in this disease remain to be clarified. Our understanding of PXE has been improved by the development of transgenic mouse models by specifically inactivating the *Abcc6* gene (Klement et al., 2005; Gorgels et al., 2005). Consistently, *Abcc6*^{-/-} mice recapitulate several histopathological findings typical of PXE patients, including the slowly progressive mineralization of connective tissues in the skin, eyes and the arterial blood vessels (Klement et al., 2005; Jiang et al., 2007). The aim of this study was to investigate fibroblasts isolated from the skin of *Abcc6*^{-/-} and *Abcc6*^{+/+} mice. Moreover, animals of two different ages were used in order to compare the behavior of cells before and after the onset of calcification. The present study design can identify changes which, when preceding ectopic mineralization, could contribute to the development of pathologic calcification, as well as differences that, when observed after the occurrence of mineralization, are possibly induced by the modified environment. In order to exclude changes simply related to the animal's aging, we have compared age-matched WT and KO mice (Table 1). The choice of this model was predicated upon a number of reasons: a) The mouse model allows the analysis of cells from tissues before animals with the *Abcc6*^{-/-} genotype develop calcification, a condition that cannot be evaluated in humans since the histopathological diagnosis of PXE is routinely made after the onset of clinical manifestations, i.e., when the mineral precipitates are already present in tissues; b) Fibroblasts are an excellent model for studying PXE, since they maintain in vitro a pathological phenotype (Quaglino et al., 2000, Quaglino et al., 2005)

exhibiting oxidative stress parameters (Pasquali-Ronchetti et al., 2006) and an altered protein profile (Boraldi et al., 2009, 2013). In this study, we have investigated the occurrence of oxidative stress and the expression of a number of proteins that are involved in the calcification process and in particular in phosphate-related pathways, as we have hypothesized that they play a key role in the development and/or progression of soft connective tissue calcification in PXE (Boraldi et al., 2013; Li et al., 2012; Li et al., 2013). Our results demonstrated that murine dermal fibroblasts, in contrast to human dermal fibroblasts (Boraldi et al., 2010), exhibit in vitro morphological features and proliferative capabilities that vary dependent on the animal's age, independently of the genotype. Therefore, the absence of the *Abcc6* gene activity does not affect the proliferation potential of mesenchymal cells.

Replicative senescence in many in vitro models, including dermal fibroblasts, has been associated with increased ROS content (Lawless et al., 2012). Altered redox balance is a frequent condition common to many disorders, both in the absence or in the presence of ectopic calcification (Byon et al., 2008) and has been demonstrated to be related to the severity of clinical manifestations in patients with PXE and PXE-like disorders (Garcia et al., 2008; Boraldi et al., 2013). Since only fibroblasts from adult *Abcc6*^{-/-} mice were shown to have higher levels of O₂⁻, oxidative stress is likely the consequence of the calcified environment. Consistent with this conclusion, it has been demonstrated in the PXE animal model that antioxidant treatment can ameliorate the redox balance, without affecting the extent of mineralization (Li et al., 2008).

Bmp2 expression is essential for osteoblastic differentiation of mesenchymal cells and therefore it has been widely implicated in the development of vascular calcification (Derwall et al., 2012). Recent studies have shown that BMP2 is upregulated by ROS, being at the same time an inducer of ROS accumulation (Mandal et al., 2011) and favoring alkaline phosphatase activity and phosphate accumulation (Rawadi et al., 2003). In accordance, we have shown that *Bmp2*, in association with ectopic calcification and with ROS accumulation, is significantly upregulated in fibroblasts from adult *Abcc6*^{-/-} mice. Therefore, these data support the hypothesis that when calcification is initiated,

there is a stimulatory loop that further increases mineral deposition and alters the phenotypic behavior of fibroblasts. A key question relates to the factor(s) that are capable of triggering the initial phase of ectopic calcification in specific areas of soft connective tissues. We have already demonstrated that Tnap activity is significantly upregulated in fibroblasts from PXE patients, suggesting that phosphate metabolism plays a role in the pathogenesis of elastic fiber calcification (Boraldi et al., 2013). Present data further indicate that there is an age-dependent upregulation of Tnap expression and Tnap activity in fibroblasts from *Abcc6*^{-/-} mice. Alkaline phosphatase acts on phosphate-containing substrates by releasing Pi that can accumulate in the extracellular matrix and, under favorable conditions of the microenvironment, can precipitate in the form of hydroxyapatite crystals. One of these substrates is the calcification inhibitor, inorganic pyrophosphate (PPi), which is generated by *Enpp1* through hydrolysis of ATP to AMP and PPi, and transported to the extracellular milieu by Ank. Assessment of the expression of these proteins indicated that both the age and the genotype of mice contribute to phenotypic changes of the fibroblasts.

In particular, our data demonstrated that, at all time points, *Abcc6*^{-/-} fibroblasts have a lower expression of Ank, a protein that is necessary for providing the extracellular environment with adequate amounts of physiological calcification inhibitors, including PPi. When Ank is downregulated, soft connective tissue becomes increasingly prone to mineralization. As this process gradually progresses with increased age of the animals, fibroblasts are modified towards a phenotype that favors mineral precipitation (i.e., lower *Enpp1* and increased Tnap expression and activity). These observations are in agreement with the concept that ectopic calcification is more frequently observed in aged individuals.

Interestingly, besides PPi, other factors control mineral deposition in the extracellular matrix, including osteopontin, a well known inhibitor of vascular calcification (Scatena et al., 2007), as it regulates apatite crystal size and growth most likely by its ability to directly bind to specific apatite crystal faces (Speer et al., 2002). The marked down-regulation of *Opn* expression observed in fibroblasts from *Abcc6*^{-/-} mice at all ages, together with lower PPi availability and a progressive

1 Tnap-mediated release of Pi from the PPi pool in older mice, may act in synergy to promote mineral
2 deposition.
3

4
5
6 In this study, a comparison of a number of parameters, before and after the onset of mineral
7 deposition in tissues of PXE mice, demonstrated that there are changes in dermal fibroblasts that
8 can be related to the genotype and that are present well before the development of calcification.
9 Such changes possibly represent a trigger of calcification, whereas other changes may reflect a
10 cellular response to the calcified environment that further sustains the mineralization process.
11 Finally, the observation that Ank expression is significantly reduced in fibroblasts from the young
12 Abcc6^{-/-} mice supports the hypothesis that phosphate metabolism is locally altered in PXE (Boraldi
13 et al., 2013) and that reduced transport of the calcification inhibitor PPi in the extracellular
14 compartment, together with impaired carboxylation of Matrix Gla Protein (Gheduzzi et al., 2007; Li
15 Q et al., 2007; Boraldi et al., 2013), may be the key players for the initial deposition of mineral
16 precipitates in the absence of Abcc6 transport activity.
17

18
19 In conclusion, our data demonstrate that, although grown in optimal culture conditions, dermal
20 fibroblasts from KO mice, similar to human PXE fibroblasts, exhibit and maintain in vitro
21 characteristics. Therefore, at least few of the differences in protein expression are related to the
22 genotype, whereas others parameters are modulated both by the genotype and by the age of the
23 animals (Table 1). Although it cannot be excluded that circulating factors in vivo exert an
24 epigenetic modulation on fibroblasts' phenotype, the present data support the role of mesenchymal
25 cells, such as fibroblasts in the mineralization process. These cells exhibit a differential expression
26 of molecules related to the calcification process before ectopic calcification takes place within
27 tissues, thus excluding that these changes are the consequence of the mineralized environment.
28
29 Within this context Ank and Opn may represent two potential pharmacologic targets warranting
30 further investigation in the search for novel therapies for PXE.
31
32

33
34
35
36
37
38
39
40
41
42
43
44
45
46
47
48
49
50
51
52
53
54
55
56
57 **Materials and Methods**
58
59
60

Cells

Dermal fibroblast cultures were obtained from the whole skin of 37 *Abcc6*^{-/-} and 29 *Abcc6*^{+/+} mice of 0.5 (n=27) and 12 months (n=39) of age. The study was approved by the Ethical Committee of the University of Modena and Reggio Emilia. Fibroblasts were cultured in DMEM (Gibco, Grand Island, New York, USA) with 10% fetal bovine serum (FBS) (Lonza) and used at 2nd or 3rd passages. During all experimental procedures, fibroblasts were pooled from several animals of the same age and genotype. Cells were routinely cultured in 75cm² flasks (Nunc, Roskilde, Denmark) with DMEM supplemented with 10% FBS, penicillin 100 IU/ml, streptomycin 100 µg/ml and nonessential amino acids 1X (Gibco). Cells were observed by phase contrast microscopy.

Flow Cytometry

ROS analysis was performed on proliferating cells as previously described (Boraldi et al., 2009). Briefly, cells were stained with dihydroethidium (DH₂, 1 mM) and 2',7'-dichlorodihydrofluorescein diacetate (H₂DCF-DA, 2 mM) probes (Molecular Probes, Eugene, OR) for the determination of superoxide anion O₂^{•-} and hydrogen peroxide (H₂O₂), respectively. Cells were analyzed on an EPICS XL flow cytometer (Coulter, USA) at the emission wavelengths of 575 and 520 nm. Ten thousand events were collected and evaluated for each treatment using a WINMDI 2.8 program. Experiments were performed in duplicate and repeated twice.

Western blot

Cells were homogenized in RIPA buffer with protease inhibitors (Sigma), centrifuged and supernatants collected and stored at -80°C until analysis. Protein concentration was measured in each sample according to Bradford assay (Bradford, 1976) in order to load equal amounts of protein. After separation by 1D PAGE, proteins were transferred to nitrocellulose and incubated with anti-Ank, anti-Opn, anti-Bmp2 (Abcam, Cambridge-UK); anti-Enpp1; anti-Tnap (Vascular Products, Maastricht, The Netherlands), followed by appropriate horseradish peroxidase (HRP)-

conjugated secondary antibodies (Abcam). Experiments were performed at least two times with all different cell lines.

Alkaline phosphatase activity

Fibroblasts were detached by enzymatic treatment and washed three times with PBS. Cells were lysed by appropriate buffer containing 0.1% Triton X-100 (Sigma). Cell lysate (20 µL) was mixed with 100 µL Tris-glycine buffer, pH 10.3 (50 mM Tris-HCl, 100 mM glycine and 2 mM MgCl₂) and 100 µL of p-nitrophenyl phosphate (Sigma). The reaction mix was incubated at 37°C for 30 min and the reaction stopped by adding 50 µL of 3 M NaOH. Absorbance was measured at 405 nm in a microplate reader. Enzymatic activity was normalized to total protein concentration using bovine serum albumin as a standard for the Bradford protein detection method (Bradford, 1976). Control samples were set as 1. Experiments were performed three times in duplicate.

Data analysis

Data were expressed as mean values ± SD of all measurements and compared by Mann Whitney or by Anova test with significance at p<0.05. Statistical data were obtained using GraphPad software 5.0 (San Diego, CA, USA).

Conflict of interests

Authors declare no conflict of interest

Acknowledgements

Authors thank the staff of CSSI (UniMoRe) for their valuable help in animal care. This work has been supported by grant from FCRM – EctoCal (DQ) and by NIH/NIAMS grant R01AR28450 (JU).

References

- Bergen AA, Plomp AS, Schuurman EJ et al (2000). Mutations in ABCC6 cause Pseudoxanthoma elasticum. *Nat Genet* 25: 228-231.
- Boraldi F, Annovi G, Vermeer C et al (2013). Matrix Gla Protein and alkaline phosphatase are differently modulated in human dermal fibroblasts from PXE patients and controls. *J Invest Dermatol* 133: 946-954.
- Boraldi F, Annovi G, Tiozzo R et al (2010). Comparison of ex-vivo and in-vitro human fibroblast ageing models. *Mech Ageing Dev* 131: 625-635.
- Boraldi F, Annovi G, Guerra D et al (2009). Fibroblast protein profile analysis highlights the role of oxidative stress and vitamin K recycling in the pathogenesis of pseudoxanthoma elasticum. *Proteomics Clin Appl* 3: 1084-1098.
- Bradford MM (1976). A rapid and sensitive method for the quantitation of microgram quantities of protein utilizing the principle of protein-dye binding. *Anal Biochem* 72: 248-254.
- Byon CH, Javed A, Dai Q et al (2008). Oxidative stress induces vascular calcification through modulation of the osteogenic transcription factor Runx2 by AKT signaling. *J Biol Chem* 283: 15319- 15327.
- Contri MB, Boraldi F, Taparelli F et al (1996). Matrix proteins with high affinity for calcium ions are associated with mineralization within the elastic fibers of pseudoxanthoma elasticum dermis. *Am J Pathol* 148:569-577.
- Derwall M, Malhotra R, Lai CS et al (2012). Inhibition of bone morphogenetic protein signaling reduces vascular calcification and atherosclerosis. *Arterioscler Thromb Vasc Biol* 32: 613-622.
- Garcia-Fernandez MI, Gheduzzi D, Boraldi F et al (2008). Parameters of oxidative stress are present in the circulation of PXE patients. *Biochim Biophys Acta* 1782: 474-481.
- Gheduzzi D, Boraldi F, Annovi G et al (2007). Matrix Gla protein is involved in elastic fiber calcification in the dermis of pseudoxanthoma elasticum patients. *Lab Invest* 87: 998-1008.
- Giachelli CM (2005). Inducers and inhibitors of biomineralization: lessons from pathological

calcification. *Orthod Craniofac Res* 8: 229-231.

Gorgels TG, Hu X, Scheffer GL et al (2005). Disruption of *Abcc6* in the mouse: novel insight in the pathogenesis of pseudoxanthoma elasticum. *Hum Mol Genet* 14: 1763-1773.

Jiang Q, Li Q, Uitto J (2007). Aberrant mineralization of connective tissues in a mouse model of pseudoxanthoma elasticum: systemic and local regulatory factors. *J Invest Dermatol* 127: 1392-1402.

Klement JF, Matsuzaki Y, Jiang QJ et al (2005). Targeted ablation of the *ABCC6* gene results in ectopic mineralization of connective tissues. *Mol Cell Biol* 25: 8299-8310.

Lawless C, Jurk D, Gillespie CS et al (2012). A stochastic step model of replicative senescence explains ROS production rate in ageing cell populations. *PLoS One* 7: e32117.

Le Saux O, Urban Z, Tschuch C et al (2000). Mutations in a gene encoding an ABC transporter cause pseudoxanthoma elasticum. *Nat Genet* 25: 223-227.

Le Saux O, Bunda S, VanWart CM et al (2006). Serum factors from pseudoxanthoma elasticum patients alter elastic fiber formation in vitro. *J Invest Dermatol* 126: 1497-1505.

Li Q, Brodsky JL, Conlin LK et al (2013). Mutations in the *ABCC6* gene as a cause of generalized arterial calcification of infancy: Genotypic overlap with pseudoxanthoma lasticum. *J Invest Dermatol* 5. doi: 10.1038.

Li Q, Schumacher W, Jablonski D et al (2012). Cutaneous features of pseudoxanthoma elasticum in a patient with generalized arterial calcification of infancy due to a homozygous missense mutation in the *ENPP1* gene. *Br J Dermatol* 166: 1107-1111.

Li Q, Jiang Q, Pfindner E et al (2008). Pseudoxanthoma elasticum: clinical phenotypes, molecular genetics and putative pathomechanisms. *Exp Derm* 18: 1-11.

Li Q, Jiang Q, Schurgers LJ et al (2007). Pseudoxanthoma elasticum: reduced gamma-glutamyl carboxylation of matrix gla protein in a mouse model (*Abcc6*^{-/-}). *Biochem Biophys Res Commun* 364: 208-213.

Li Q, Jiang Q, Uitto J. (2008). Pseudoxanthoma elasticum: oxidative stress and antioxidant diet in a mouse model (*Abcc6*^{-/-}). *J Invest Dermatol* 128:1160-1164

- Mandal CC, Ganapathy S, Gorin Y et al (2011). Reactive oxygen species derived from Nox4 mediate BMP2 gene transcription and osteoblast differentiation. *Biochem J* 433: 393-402.
- Pasquali-Ronchetti I, Garcia-Fernandez MI, Boraldi F et al (2006). Oxidative stress in fibroblasts from patients with pseudoxanthoma elasticum: possible role in the pathogenesis of clinical manifestations. *J Pathol* 208: 54-61.
- Passi A, Albertini R, Baccarani Contri M et al (1996). Proteoglycan alterations in skin fibroblast cultures from patients affected with pseudoxanthoma elasticum. *Cell Biochem Funct* 14: 111-120.
- Quaglino D, Boraldi F, Annovi G et al (2011). The multifaceted complexity of genetic diseases: a lesson from Pseudoxanthoma Elasticum. In: *Advances in the study of genetic disorders*. (Ikehara K, editor) Rijeka, Croazia: in Tech, 289-318.
- Quaglino D, Sartor L, Garbisa S et al (2005). Dermal fibroblasts from pseudoxanthoma elasticum patients have raised MMP-2 degradative potential. *Biochim Biophys Acta* 1741: 42-47.
- Quaglino D, Boraldi F, Barbieri D et al (2000). Abnormal phenotype of in-vitro dermal fibroblasts from patients with pseudoxanthoma elasticum (PXE). *Biochim Biophys Acta* 1501: 51-62.
- Rawadi G, Vayssi.re B, Dunn F et al (2003). BMP-2 controls alkaline phosphatase expression and osteoblast mineralization by a Wnt autocrine loop. *J Bone Miner Res* 18: 1842-1853.
- Ringpfeil F, Lebowhl MG, Christiano AM et al (2000). Pseudoxanthoma elasticum: mutations in the MRP6 gene encoding a transmembrane ATP-binding cassette (ABC) transporter. *Proc. Natl Acad Sci USA* 91: 6001-6006.
- Ronchetti I, Boraldi F, Annovi G et al (2013). Fibroblast involvement in soft connective tissue calcification. *Front Genet.* 4:22.
- Scatena M, Liaw L, Giachelli CM (2007). Osteopontin: a multifunctional molecule regulating chronic inflammation and vascular disease. *Arterioscler Thromb Vasc Biol* 27:2302-2309.
- Speer MY, McKee MD, Guldberg RE et al (2002). Inactivation of the osteopontin gene enhances vascular calcification of matrix Gla protein-deficient mice: evidence for osteopontin as an inducible inhibitor of vascular calcification in vivo. *J Exp Med* 196:1047-1055.

Table 1: Influence of genotype (WT vs KO) and aging (0.5 vs 12 months) on the expression of cellular parameters.

Parameters		CHANGES INFLUENCED BY	
		Genotype	Age
O ₂	content	YES	YES
Bmp2	expression	YES	YES
Tnap	expression	NO	YES
	activity	YES	YES
Enpp1	expression	NO	YES
Ank	expression	YES	NO
Opn	expression	YES	NO

Legend to figures

Figure 1. Dermal fibroblasts cultured from KO (Abcc6^{-/-}) and WT (Abcc6^{+/+}) mice of 0.5 and 12 months of age and observed by phase contrast microscopy (A). Differences in the proliferation capabilities are related to the age of the animals, but are independent of the genotype as clearly shown in graph (B). Bar = 300 μ m.

Figure 2. Anion superoxide (O₂⁻) and hydrogen peroxide (H₂O₂) content measured by flow cytometry in dermal fibroblasts cultured from WT (Abcc6^{+/+}) and KO (Abcc6^{-/-}) mice of 0.5 and 12 months of age. *p<0.05, KO vs WT of the same age; # p<0.05 0.5 vs 12 months of age within the same genotype.

Figure 3. Expression of Bmp2 measured by Western blot in dermal fibroblasts cultured from WT (Abcc6^{+/+}) and KO (Abcc6^{-/-}) mice of 0.5 and 12 months of age. Data are expressed as mean values \pm SD of densitometric analyses were values in cells from WT animals 0.5 month-old were set at 1. A representative Western blot is shown. *p<0.05, KO vs WT of the same age; ## p<0.01, 0.5 vs 12 months within the same genotype.

Figure 4. Tnap expression and activity were evaluated in dermal fibroblasts cultured from WT (Abcc6^{+/+}) and KO (Abcc6^{-/-}) mice of 0.5 and 12 months of age. Data are expressed as mean values \pm SD of different measurements were values in cells from WT animals 0.5 month-old were set at 1. A representative Western blot is shown. *p<0.05, KO vs WT of the same age; ## p<0.01 and ### p<0.001, 0.5 vs 12 months within the same genotype.

Figure 5. Enpp1 and Ank expression measured by Western blot in dermal fibroblasts cultured from WT (Abcc6^{+/+}) and KO (Abcc6^{-/-}) mice of 0.5 and 12 months of age. Data are expressed as mean values \pm SD of densitometric analyses were values in cells from WT animals 0.5 month-old were

1
2
3
4
5
6
7
8
9
10
11
12
13
14
15
16
17
18
19
20
21
22
23
24
25
26
27
28
29
30
31
32
33
34
35
36
37
38
39
40
41
42
43
44
45
46
47
48
49
50
51
52
53
54
55
56
57
58
59
60

set at 1. Representative Western blots are shown. **p<0.01 KO vs WT of the same age; ### p<0.01 0.5 vs 12 months within the same genotype.

Figure 6. Expression of Opn measured by Western blot in dermal fibroblasts cultured from WT (Abcc6^{+/+}) and KO (Abcc6^{-/-}) mice of 0.5 and 12 months of age. Data are expressed as mean values ± SD of densitometric analyses were values in cells from WT animals 0.5 month-old were set at 1. A representative Western blot is shown. *p<0.05 and **p<0.01 KO vs WT of the same age.

For Review Only

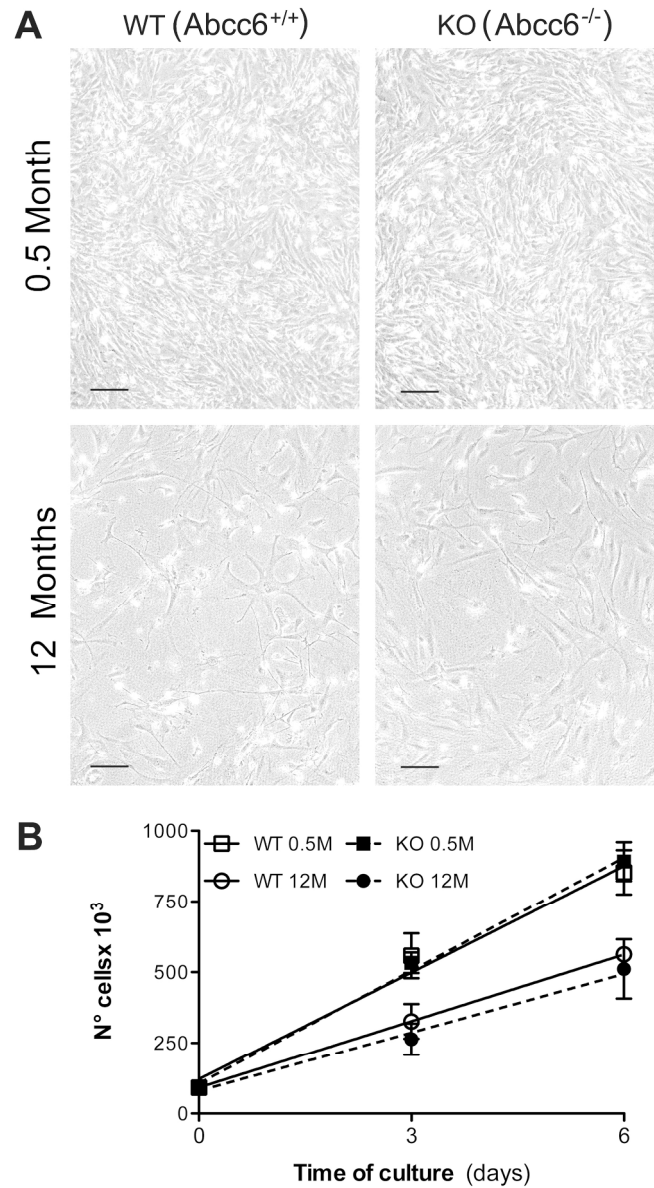


Figure 1
155x282mm (300 x 300 DPI)

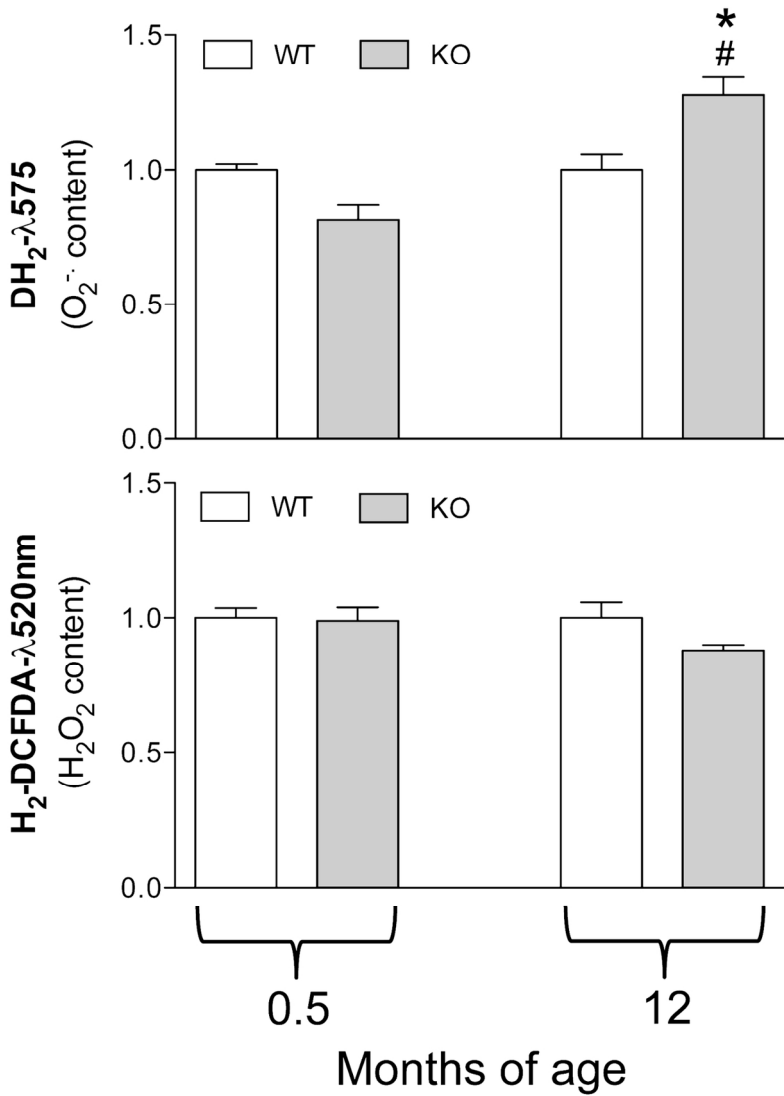


Figure 2
124x181mm (300 x 300 DPI)

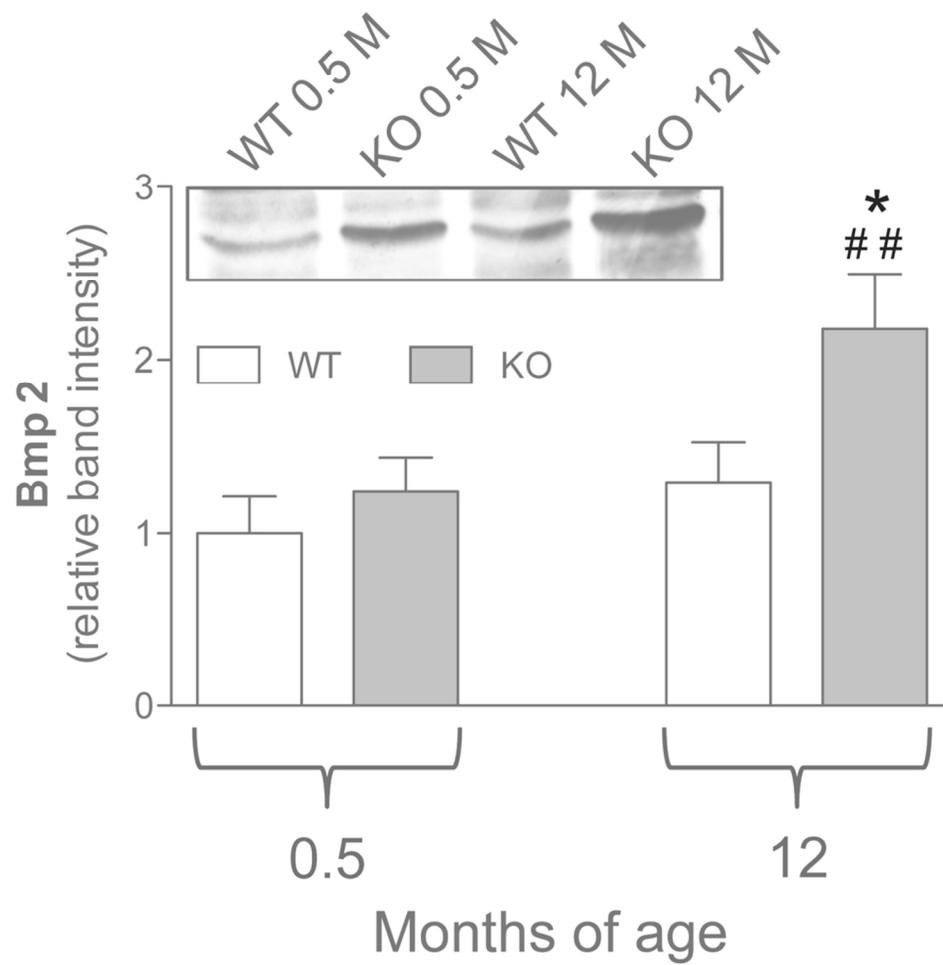


Figure 3
87x89mm (300 x 300 DPI)

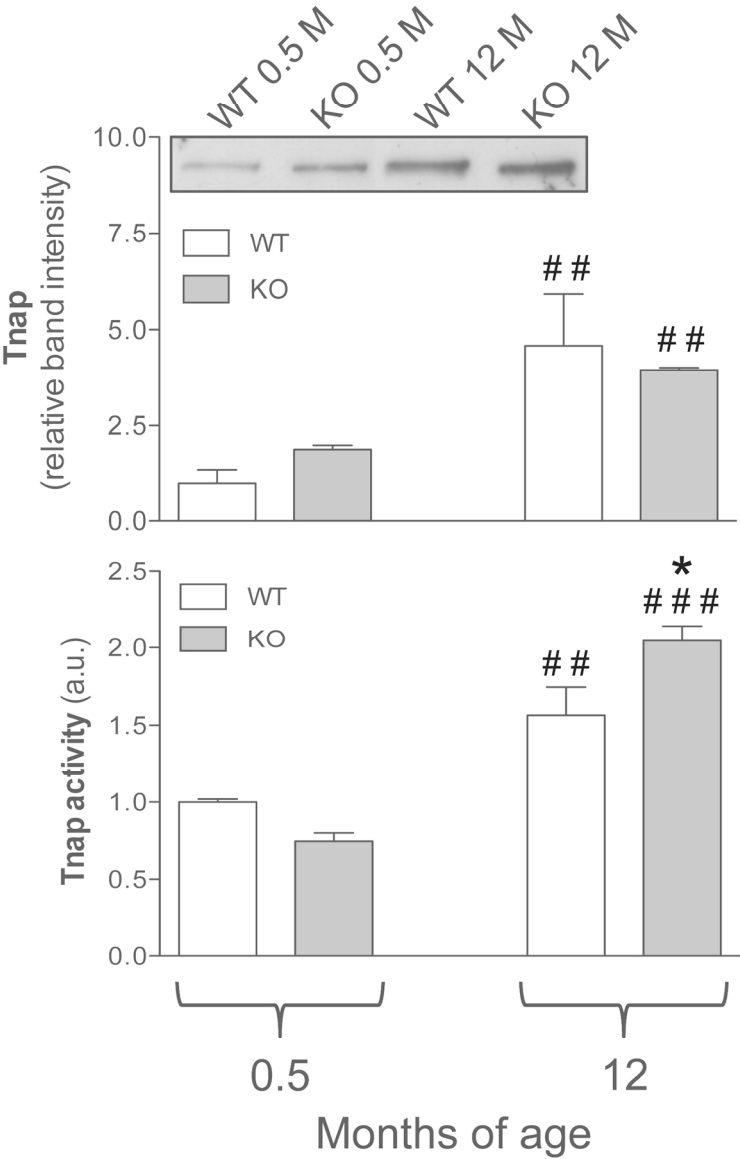


Figure 4
133x208mm (300 x 300 DPI)

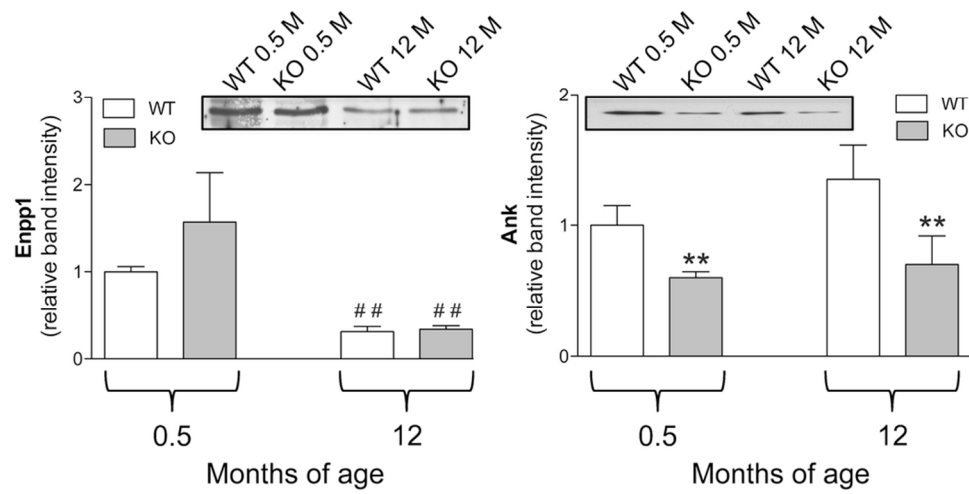


Figure 5
91x48mm (300 x 300 DPI)

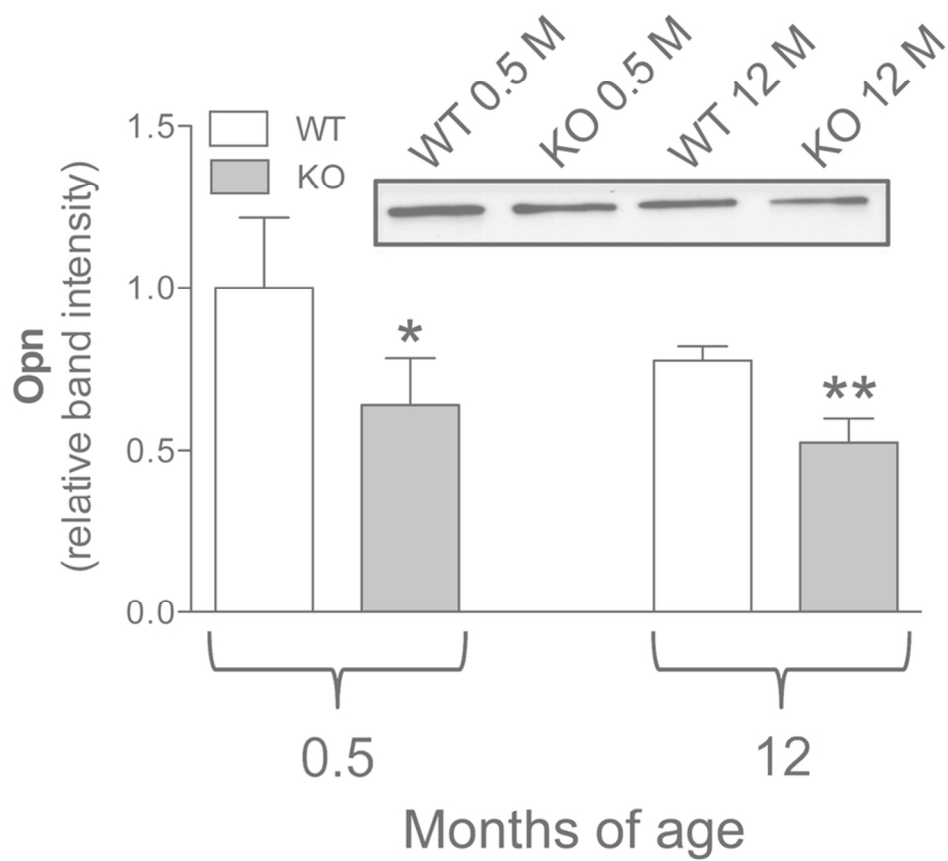


Figure 6
79x74mm (300 x 300 DPI)